Transactions Papers

Generalized Raised-Cosine Filters

Nader Sheikholeslami Alagha and Peter Kabal, *Member, IEEE*

***Abstract*— Data transmission over bandlimited channels requires pulse shaping to eliminate or control intersymbol interference (ISI). Nyquist filters provide ISI-free transmission. Here we introduce a phase compensation technique to design Nyquist filters. Phase compensation can be applied to the square-root of any zero-phase bandlimited Nyquist filter with normalized excess bandwidth less than or equal to one. The resulting phase compensated square-root filter is also a Nyquist filter. In the case of a raised-cosine spectrum, the phase compensator has a simple piecewise-linear form. Such a technique is particularly useful to accommodate two different structures for the receiver, one with a filter matched to the transmitting filter and one without a matched filter.**

We also use the phase compensation technique to characterize a more general family of Nyquist filters which subsumes raised-cosine spectra. These generalized raised-cosine filters offer more flexibility in filter design. For instance, the rate of asymptotic decay of the filter impulse response may be increased, or the residual ISI, introduced by truncation of the impulse response, may be minimized. Design examples are provided to illustrate these choices.

***Index Terms*— Data transmission, intersymbol interference, Nyquist filters, pulse amplitude modulation.**

I. Introduction

A CONVENTIONAL baseband pulse amplitude modulation (PAM) signal can be represented as

$$x(t) = \sum_{k=-\infty}^{\infty} a_k g(t - kT_s) \tag{1}$$

where a_k's are the transmitted symbols and $g(\cdot)$ is a real-valued "Nyquist pulse" which satisfies Nyquist's first criterion

$$g(kT_s) = \begin{cases} 1, & \text{for } k = 0 \\ 0, & \text{for } k = \pm 1, \pm 2, \cdots. \end{cases} \tag{2}$$

$g(\cdot)$ represents the overall impulse response of the transmitting filter, receiving filter, and the communication channel. Each transmitted symbol a_k can be recovered from the received signal $x(t)$, by taking samples of $x(t)$ at the time instances kT_s. In other words, choosing $g(\cdot)$ as a Nyquist pulse avoids intersymbol interference (ISI), and allows sample-by-sample detection at the receiver. In the frequency domain, Nyquist's first criterion is written as

$$\sum_{n=-\infty}^{\infty} G\left(f - \frac{n}{T_s}\right) = T_s \tag{3}$$

where $G(f)$ is known as a Nyquist filter. A particular Nyquist filter with wide practical applications is the *raised-cosine* filter

$$G_{rc}(f) = \begin{cases} T_s, & |f| \le \dfrac{1-\alpha}{2T_s} \\ T_s \cos^2\left(\dfrac{\pi T_s}{2\alpha}\left(|f| - \dfrac{1-\alpha}{2T_s}\right)\right), & \dfrac{1-\alpha}{2T_s} \le |f| \le \dfrac{1+\alpha}{2T_s} \\ 0, & |f| > \dfrac{1+\alpha}{2T_s} \end{cases} \tag{4}$$

where α is called the *roll-off factor* and takes values between zero and one. The parameter α also represents the normalized *excess bandwidth* occupied by the signal beyond the Nyquist frequency $1/2T_s$.

In practical applications, the overall magnitude response of the Nyquist filter is split evenly between the transmitter and receiver. The phase response of the receiving filter compensates for the transmitting filter phase so that the overall filter has a linear phase

$$\begin{aligned} G(f) &= G_T(f) G_R(f) \\ |G_T(f)| &= |G_R(f)| = \sqrt{|G(f)|} \\ \angle G_R(f) &= -2\pi f \tau_0 - \angle G_T(f). \end{aligned} \tag{5}$$

$G_T(f)$ and $G_R(f)$ are the transfer functions of the transmitting and receiving filters accordingly. The receiving filter in this case is matched to the transmitting filter to maximize the signal-to-noise ratio (SNR) at the sampling time instances at the receiver [1]. The transmitting and receiving filters are typically considered to be linear phase with a nominal delay of $\tau_0/2$ that is required to make the filters physically realizable.

We consider more general phase responses for the transmitting and receiving filters. The phase compensated transmitting filter satisfies Nyquist's first criterion. As a result, with or without a matched filter at the receiver, we obtain ISI free transmission. The ability to use a simple receiver filter (not a

Paper approved by K. Townsend, the Editor for Computer-Aided Design of Communication Systems for the IEEE Communications Society. Manuscript received March 25, 1998; revised August 12, 1998. This work was supported by the Natural Sciences and Engineering Research Council of Canada. This paper was presented in part at the 19th Biennial Symposium on Communications, Kingston, ON, Canada, June 1998.

The authors are with the Department of Electrical and Computer Engineering, McGill University, Montreal, PQ, Canada H3A 2A7, Canada (e-mail: Kabal@ece.mcgill.ca; Nader@ece.mcgill.ca).

Publisher Item Identifier S 0090-6778(99)05232-0.

matched filter) is particularly useful to reduce the cost of the receiver [2]. There are also new voice-band modems designed for PCM channels where the channel at one end is terminated to the digital telephone network [3]–[5]. Since there is no access to the filters at the telephone network, the pulse shaping should be performed entirely at the other end (analog end user). The phase compensation technique, as it will be described here, provides a method to perform pulse shaping at one end of the channel and, at the same time, stay compatible with the other structures where a matched filter is in place at the receiver.

In Section II, a general relationship between phase and amplitude responses of a bandlimited Nyquist filter is presented. We show that a bandlimited zero-phase Nyquist filter can always be split into two cascaded Nyquist filters matched to one another. The special case of the square-root raised-cosine spectrum is investigated. We quantify the SNR degradation due to replacing the matched filter by a lowpass filter.

In Section III, a bandlimited Nyquist filter with excess bandwidth less than or equal to one is characterized by a phase compensator. A general family of Nyquist filters is introduced which includes the standard raised-cosine filters. The square-root of the generalized raised-cosine filter can be phase compensated to become a Nyquist filter. Some examples of Nyquist filter design are presented.

II. Extension of Nyquist's First Criterion

The transfer function of a filter $G(f)$ with real impulse response $g(t)$ can be expressed in terms of its magnitude and phase responses

$$G(f) = |G(f)| \cdot e^{j\phi(f)} \tag{6}$$

where $\phi(\cdot)$ is a real-valued odd function and $|G(\cdot)|$ is a real-valued function with even symmetry. In our discussion we assume $G(f)$ is bandlimited to $|f| < 1/T_s$. We consider the relationship between $|G(f)|$ and $\phi(f)$ such that $G(f)$ satisfies Nyquist's first criterion. For a Nyquist filter with normalized excess bandwidth less than or equal to one, Nyquist's first criterion is written as

$$|G(f)| \cdot e^{j\phi(f)} + |G(f-1/T_s)| \cdot e^{j\phi(f-1/T_s)} = K, \quad 0 \le f \le \frac{1}{T_s} \tag{7}$$

where K is a real constant. Following Gibby and Smith [6], we decompose (7) into the real and imaginary parts

$$|G(f)| \cdot \cos\,\phi(f) + |G(f-1/T_s)| \cdot \cos\,\phi(f-1/T_s) = K \tag{8}$$

$$|G(f)| \cdot \sin\,\phi(f) + |G(f-1/T_s)| \cdot \sin\,\phi(f-1/T_s) = 0. \tag{9}$$

As shown in [6], one can combine (8) and (9) to express $\phi(f)$ in terms of the magnitude response of $G(f)$

$$\phi(f) = \arccos\left(\frac{K^2 + |G(f)|^2 - |G(f-1/T_s)|^2}{2K|G(f)|}\right), \quad 0 \le f \le \frac{1}{T_s}. \tag{10}$$

Note that for $-1/T_s \le f \le 0$ the phase response $\phi(f)$ is determined using its odd symmetry property $\phi(-f) = -\phi(f)$. Since the argument of the $\arccos(\cdot)$ should be limited to one in absolute value, there may not be a real solution for $\phi(f)$.

A. Square-Root Nyquist Filters

For the case of a zero-phase Nyquist filter, we can design a phase compensator for the square-root filter such that the compensated square-root filter also satisfies Nyquist's criterion. To show this, consider the zero-phase Nyquist filter $|G(f)|^2$

$$|G(f)|^2 + |G(f-1/T_s)|^2 = T_s, \qquad 0 \le f \le \frac{1}{T_s}. \tag{11}$$

The phase compensated square-root filter is

$$G(f) = |G(f)| \cdot e^{j\theta(f)}. \tag{12}$$

The phase compensator $\theta(f)$ is chosen such that $G(f)$ is Nyquist filter. From (10), $\theta(f)$ can be expressed in terms of $|G(f)|$ as

$$\theta(f) = \arccos\left(\frac{A^2 + |G(f)|^2 - |G(f-1/T_s)|^2}{2A|G(f)|}\right), \quad 0 \le f \le \frac{1}{T_s} \tag{13}$$

where A is a real constant. If we choose $A = \sqrt{T_s}$, the phase compensator simplifies

$$\theta(f) = \arccos\left(\frac{|G(f)|}{\sqrt{T_s}}\right), \qquad 0 \le f \le \frac{1}{T_s}. \tag{14}$$

From (11) it is evident that $0 \le |G(f)|/\sqrt{T_s} \le 1$. Therefore, there is always a real solution for $\theta(f)$ in (14).

The phase compensator can fully characterize the zero-phase Nyquist filter and the phase compensated square-root filter

$$|G(f)|^2 = T_s \cos^2\,\theta(f) \tag{15}$$

$$G(f) = \sqrt{T_s}\,\cos\,\theta(f) \cdot e^{j\theta(f)}. \tag{16}$$

Note that $|G(f)|^2$ is to within a scaling factor, the real part of $G(f)$

$$|G(f)|^2 = \sqrt{T_s}\,\mathrm{Re}[G(f)]. \tag{17}$$

B. Phase Compensated Square-Root Raised-Cosine Filter

The standard raised-cosine spectrum as defined in (4) is zero phase and satisfies Nyquist's criterion. To find the phase compensator $\theta(f)$, we substitute the square-root of the raised-cosine spectrum into (14). The resulting phase response $\theta(f)$ is a piecewise-linear function, as shown in Fig. 1 and expressed below

$$\theta(f) = \begin{cases} \dfrac{\pi T_s}{2\alpha}\left(-f - \dfrac{1-\alpha}{2T_s}\right), & \text{for } -\dfrac{1+\alpha}{2T_s} \le f \le -\dfrac{1-\alpha}{2T_s} \\ 0, & \text{for } |f| < \dfrac{1-\alpha}{2T_s} \\ \dfrac{\pi T_s}{2\alpha}\left(-f + \dfrac{1-\alpha}{2T_s}\right), & \text{for } \dfrac{1-\alpha}{2T_s} \le f \le \dfrac{1+\alpha}{2T_s}. \end{cases} \tag{18}$$

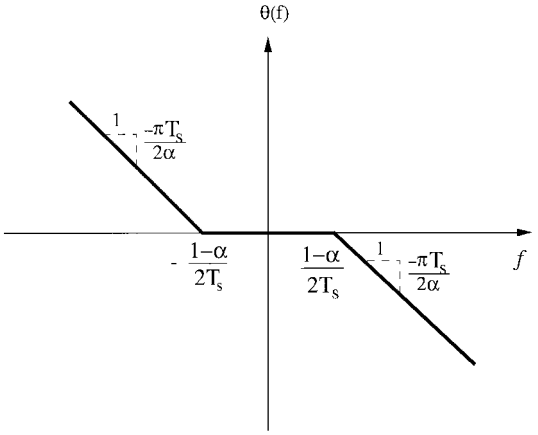

Fig. 1. Piecewise linear phase compensator for square-root raised-cosine filter.

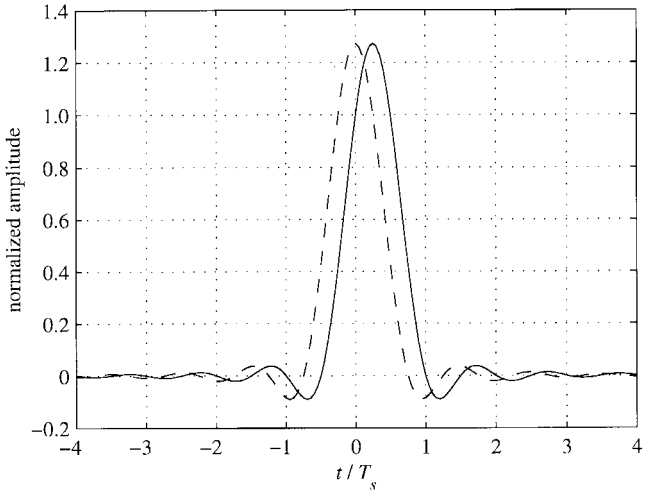

Fig. 2. Normalized impulse responses of the square-root raised-cosine filter with $\alpha = 1$ (dashed line). The phase compensated filter has a delayed impulse response (solid line).

Note that $-\theta(f)$ can also be used for phase compensation. Therefore, for the transmitting and receiving filters, we can use $G_T(f)=\sqrt{|G_{rc}(f)|}e^{j\theta(f)}$ and $G_R(f)=\sqrt{|G_{rc}(f)|}e^{-j\theta(f)}$, which are individually Nyquist filters and matched to one another. Throughout our discussion here, we assume the time delay τ_0, introduced in (5), is zero. A time delay can always be added to an appropriately truncated filter response to make it causal and physically realizable.

The impulse response of the phase-compensated square-root raised-cosine filter has a simple closed form

$$\begin{aligned} g(t) &= \mathcal{F}^{-1}\left\{\sqrt{|G_{rc}(f)|}e^{j\theta(f)}\right\} \\ &= \frac{\pi}{2\sqrt{T_s}}\operatorname{sinc}\left(\frac{t}{T_s}\right)\cdot\operatorname{sinc}\left(\frac{\alpha t}{T_s}-\frac{1}{2}\right) \end{aligned} \tag{19}$$

where $\mathcal{F}^{-1}$ is the inverse Fourier transform and $\operatorname{sinc}(x) = \sin(\pi x)/\pi x$. The filter impulse response is expressed as a product of two terms where the first term, $\operatorname{sinc}(t/T_s)$, provides the regular zero crossings at integer multiples of T_s. In general, adding the phase compensator to the square-root filter changes the filter-impulse response, and the pulse shape may no longer be symmetric.

Using the inverse Fourier transform of (17), we can show that the impulse response of a standard raised-cosine filter is within to a scaling factor the even part of $g(t)$:

$$\begin{aligned} g_{rc}(t) &= \frac{\sqrt{T_s}}{2}\left(g(t)+g(-t)\right) \\ &= \frac{\pi}{4}\operatorname{sinc}\left(\frac{t}{T_s}\right)\left(\operatorname{sinc}\left(\frac{\alpha t}{T_s}-\frac{1}{2}\right)+\operatorname{sinc}\left(\frac{\alpha t}{T_s}+\frac{1}{2}\right)\right) \end{aligned} \tag{20}$$

which is consistent with the result given in [7, p. 62].

C. Special Case: Full Excess Bandwidth

In the case of full excess bandwidth, i.e., $\alpha = 1$, $\theta(f)$ is a linear function over the whole frequency range of the filter

$$\theta(f) = -\frac{\pi T_s}{2}f, \qquad \text{for } |f| \le \frac{1}{T_s}. \tag{21}$$

The zero-phase square-root raised-cosine filter (no phase compensation) has the following impulse response

$$\mathcal{F}^{-1}\left\{\sqrt{|G_{rc}(f)|}\right\} = \frac{\pi}{2\sqrt{T_s}}\operatorname{sinc}\left(\frac{t}{T_s}+\frac{1}{4}\right)\operatorname{sinc}\left(\frac{t}{T_s}-\frac{1}{4}\right). \tag{22}$$

The zero-crossings of the impulse response do not occur in the correct places. Adding the phase response $\theta(f)$ to the filter delays the impulse response by a quarter of the sampling period T_s:

$$\mathcal{F}^{-1}\left\{\sqrt{|G_{rc}(f)|}e^{j\theta(f)}\right\} = \frac{\pi}{2\sqrt{T_s}}\operatorname{sinc}\left(\frac{t}{T_s}\right)\operatorname{sinc}\left(\frac{t}{T_s}-\frac{1}{2}\right). \tag{23}$$

Fig. 2 shows the two impulse responses where both pulses are normalized by $1/\sqrt{T_s}$. Since $\theta(f)$ causes only a pure time delay, the phase compensation does not change the pulse shape. Thus, in the case of full excess bandwidth, with or without a matched filter at the receiver, one can achieve ISI free transmission using the square-root full raised-cosine filter by merely shifting the sampling points at the receiver.

D. Eye Pattern Diagram

Eye pattern diagrams provide a simple and effective way to measure and visualize the noise immunity of a pulse shaping scheme. Using an eye pattern, one can also assess the effect of errors in the timing phase and the sensitivity to phase jitter [8]. Here, we use the eye pattern diagrams to compare conventional raised-cosine filters with the phase-compensated square-root raised-cosine filters.

First consider a raised-cosine filter with $\alpha = 1$; Fig. 3(a) shows the eye pattern of the pulse shape modulated by binary data. At integer multiples of the sampling period, each transmitted symbol can be recovered without any ISI. Fig. 3(b) shows the eye pattern of a square-root full raised-cosine spectrum. Note that the center of the eye in Fig. 3(b) coincides with peak of the impulse response. For zero ISI, the sampling

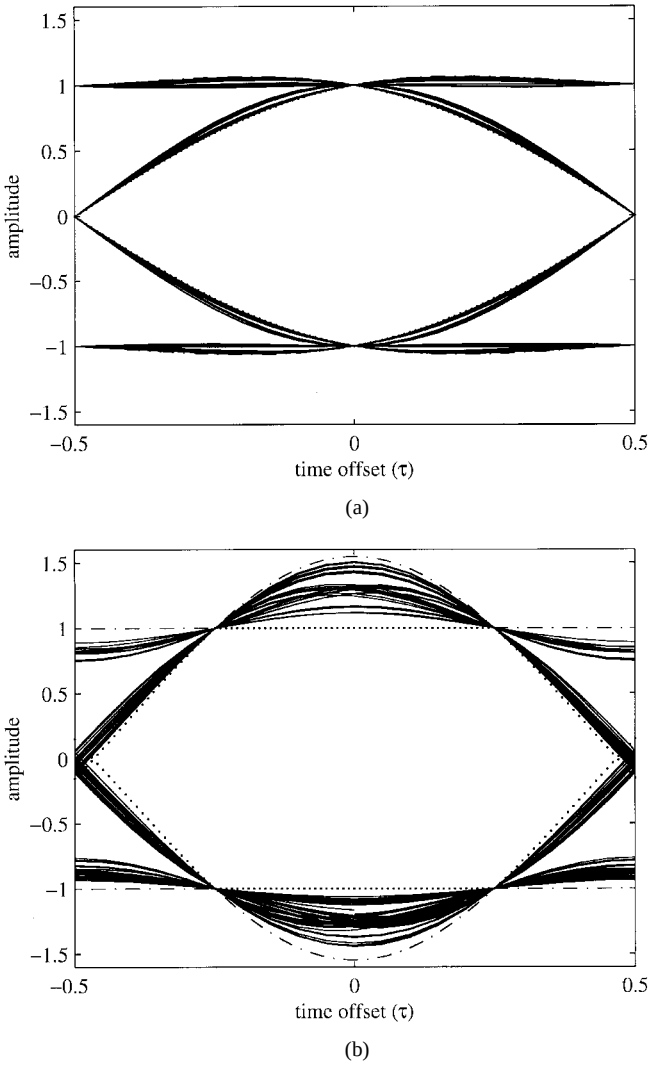

Fig. 3. Binary eye patterns for a raised-cosine filter and a square-root raised-cosine filter. (a) Raised-cosine filter with $\alpha = 1$. (b) Square-root raised-cosine filter with $\alpha = 1$.

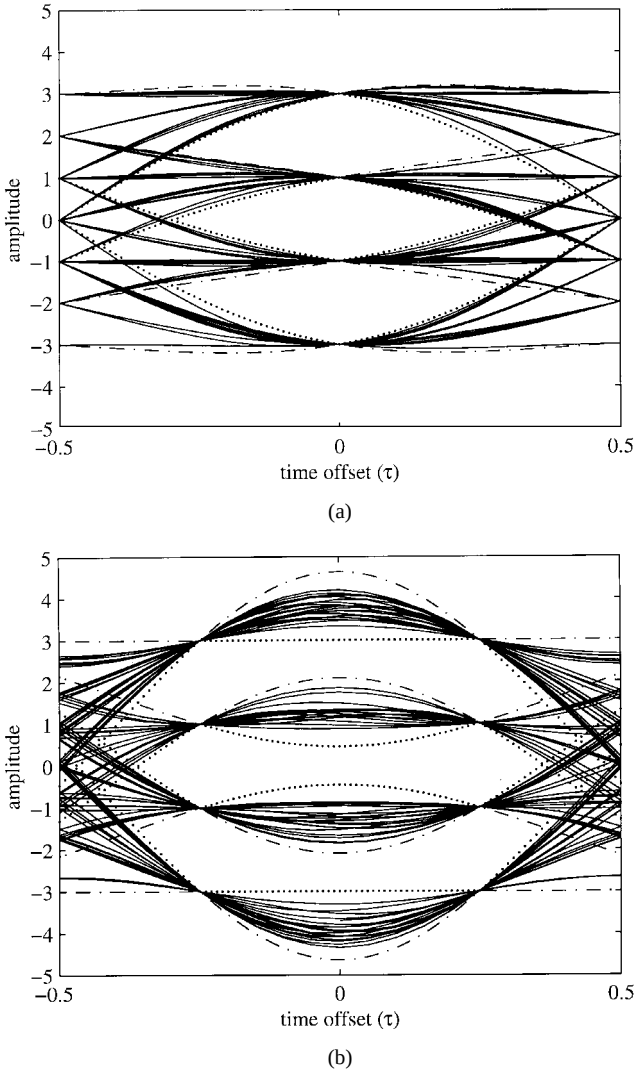

Fig. 4. Eye patterns (4-level PAM) for a raised-cosine filter and a square-root raised-cosine filter. (a) Raised-cosine filter with $\alpha = 1$. (b) Square-root raised-cosine filter with $\alpha = 1$.

points should be shifted by one quarter of sampling time. However, for the special case of binary data, the center of the eye has the widest vertical opening. In fact, in Appendix A we show that the lower boundaries of the eye pattern stay constant, equal to 1 and -1 for half of the sampling period around the center. The boundaries are shown in Fig. 3(b) as dotted lines. Compared to the eye pattern of the conventional full raised-cosine filter, the eye pattern of the square-root filter shows that it is insensitive to sampling phase error over a large interval.

Note however, that the above results are based on the binary PAM signaling and do not generalize to a multilevel PAM signaling. Fig. 4 illustrates the eye patterns of the same filters with 4-level input data. To avoid ISI, the sampling points for the square-root raised-cosine filter should be shifted by a quarter of a sampling period.

As another example, consider the raised-cosine filter with $\alpha = 0.5$. Fig. 5 shows the eye diagram for the raised-cosine and phase-compensated square-root raised-cosine filters. Due to the nonsymmetric impulse response of the filter, the eye pattern of the modified square-root raised-cosine is not symmetric around the sampling points.

E. SNR Degradation

It is well known that the use of matched filter at the receiver of an additive white Gaussian noise (AWGN) channel maximizes the signal-to-noise ratio at the sampling instants [1]. Here, we quantify the SNR degradation due to the use of a nonmatched filter at the receiver.

Assume that the transmitter uses a modified square-root raised-cosine filter. The received signal is passed through a filter $H(f)$, and is sampled at integer multiples of T_s. Let us also assume the channel adds only white Gaussian noise to the transmitted signal. The noise power at the output of the receiving filter is calculated as

$$\sigma_n^2 = \frac{N_0}{2} \int_{-\infty}^{\infty} |H(f)|^2 \, df \tag{24}$$

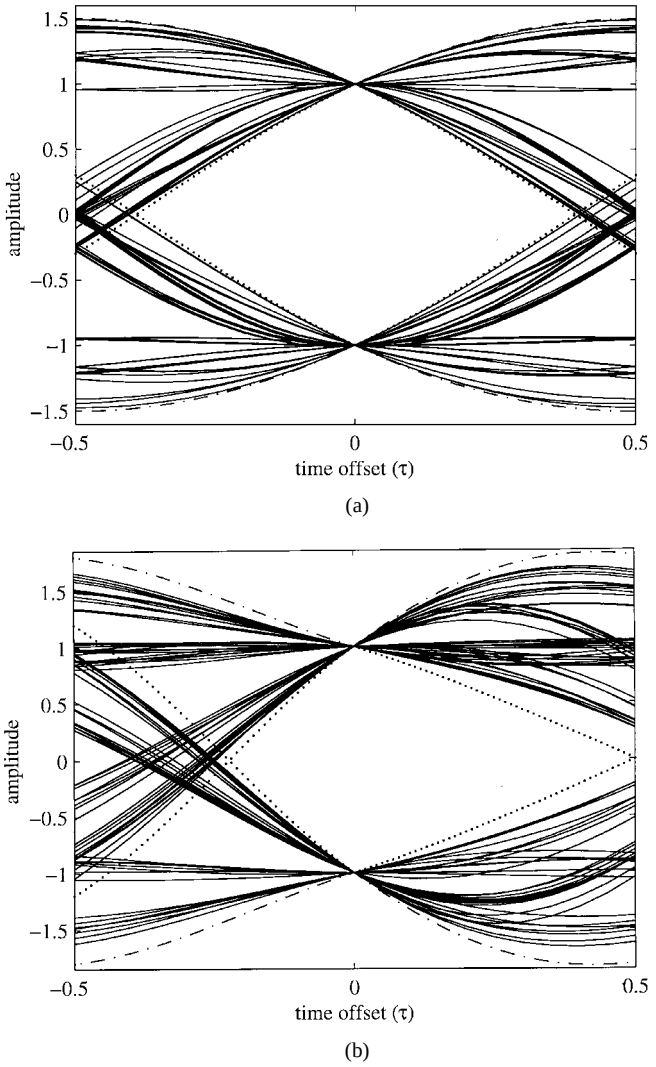

Fig. 5. Binary eye patterns for a raised-cosine filter and a phase compensated square-root raised-cosine filter. (a) Raised-cosine filter with $\alpha = 0.5$. (b) Phase-compensated square-root raised-cosine filter with $\alpha = 0.5$.

where $N_0/2$ is the power spectral density of the noise. The signal power at the sampling instance can be written as

$$\sigma_s^2 = \left| \int_{-\infty}^{\infty} G_T(f) H(f)\, df \right|^2 \tag{25}$$

where $G_T(f)$ is the transmitting filter. We consider two different receiving filters:

1) a filter-matched to the transmitting filter: $H(f) = G_T^*(f)$;
2) a brick-wall filter with a passband region $|f| \le (1+\alpha)/2T_s$.

Using the fact that the transmitting filter is normalized, the SNR after sampling is

$$\text{SNR(matched)} = \frac{2}{N_0} \tag{26}$$

$$\text{SNR(brick-wall)} = \frac{2}{(1+\alpha)N_0}. \tag{27}$$

Equations (26) and (27) show that there will be a $10 \log_{10}(1+\alpha)$ dB loss if the matched filter is replaced by an ideal brick-wall filter. For instance, for $\alpha = 0.5$ the loss is 1.76 dB.

III. Nyquist Filter Design Using Phase Compensation

In Section II, we showed how the phase and magnitude responses of a bandlimited Nyquist filter are related. Here we derive a sufficient condition for a real-valued odd function $\theta(f)$ so that the zero-phase bandlimited filter in (15) and the phase compensated square-root filter in (16) satisfy Nyquist's first criterion. Note that the filters are bandlimited to $|f| < 1/T_s$. The ISI-free condition for both filters can be expressed as

$$\sqrt{T_s}\cos\theta(f)\cdot e^{j\theta(f)} + \sqrt{T_s}\cos\theta(f-1/T_s)\cdot e^{j\theta(f-1/T_s)} = \sqrt{T_s}, \qquad 0 \le f \le \frac{1}{T_s}. \tag{28}$$

Solving for $\theta(f)$, we obtain the following condition

$$\theta(f) + \theta(1/T_s - f) = n\pi + \frac{\pi}{2}, \qquad 0 \le f \le \frac{1}{T_s} \tag{29}$$

where n is an integer. Note that we use the odd symmetry of $\theta(f)$ to obtain this result.

A. Generalized Raised-Cosine Nyquist Filters

Using the condition developed for the phase compensator in (29), we introduce a general family of Nyquist filters. The standard raised-cosine filter for any normalized excess bandwidth can be regarded as a special case of this family of filters.

Let us define a real-valued monotonic odd function $V(x)$ which satisfies the following conditions

$$\begin{aligned} V(x) &= -V(-x) \\ V(x) &= 1, \qquad x \ge 1. \end{aligned} \tag{30}$$

Consider a real-valued odd function $\phi(f) = -\phi(-f)$ defined as

$$\phi(f) = -\frac{\pi}{4} V\left(\frac{2T_s}{\alpha}\left(f - \frac{1}{2T_S}\right)\right) - \frac{\pi}{4} \qquad f \ge 0. \tag{31}$$

It can be verified that $\phi(f)$ satisfies (29). Therefore, the following filters satisfy Nyquist's first criterion

$$\begin{aligned} H_G(f) &= T_s \cos^2 \phi(f) \\ H_{\text{sqrt}}(f) &= \sqrt{T_s}\cos\phi(f) e^{j\phi(f)}. \end{aligned} \tag{32}$$

We call $H_G(f)$ a generalized raised-cosine filter. If $V(x)$ is an increasing function for $-1 < x < 1$, $H_G(f)$ corresponds to a low-pass filter with monotonically decreasing spectrum. The phase-compensated square-root of $H_G(f)$ is denoted by $H_{\text{sqrt}}(f)$. The standard raised-cosine filter, defined in (4), is a special case of $H_G(f)$, where

$$V(x) = \begin{cases} -1, & x < -1 \\ x, & -1 \le x \le 1 \\ +1, & x > +1. \end{cases} \tag{33}$$

The impulse response of $H_{\text{sqrt}}(f)$ does not have a closed form in general. In Appendix B, we show that

$$h_{\text{sqrt}}(t) = \mathcal{F}^{-1}\{H_{\text{sqrt}}(f)\} = \frac{1}{\sqrt{T_s}}\,\text{sinc}\left(\frac{t}{T_s}\right)\cdot\left(\cos\left(\frac{\pi t\alpha}{T_s}\right) + \frac{\pi\alpha t}{T_s}\int_0^1 \cos\left(\frac{\pi}{2}V(x) - \frac{\pi t\alpha}{T_s}\,x\right)dx\right). \quad (34)$$

The first term, $\text{sinc}(t/T_s)$, provides regular zero crossings at integer multiples of T_s except at $t = 0$. In the case of conventional raised-cosine filter, the impulse response has a closed form as shown in (19). In more general cases, the impulse response must be evaluated numerically. Decomposing the impulse response into two terms as shown in (34) facilitates the numerical evaluation.

The impulse response of $H_G(f)$, denoted by $h_G(t)$, is to within a scaling factor the even part of $h_{\text{sqrt}}(t)$ [see (17)]

$$h_G(t) = \frac{\sqrt{T_s}}{2}(h_{\text{sqrt}}(t) + h_{\text{sqrt}}(-t)) = \text{sinc}\left(\frac{t}{T_s}\right)\cdot\left(\cos\left(\frac{\pi t\alpha}{T_s}\right) + \frac{\pi\alpha t}{T_s}\int_0^1 \sin\left(\frac{\pi}{2}V(x)\right)\cdot\sin\left(\frac{\pi t\alpha}{T_s}\,x\right)dx\right). \quad (35)$$

B. Xia's Family of Nyquist Filters

Xia has presented a family of Nyquist filters which, with or without a matched filter at the receiver, satisfy the ISI-free conditions [2]. Each filter in this family is characterized by a real-valued continuous function $\nu(x)$ which "controls the transfer band of the filters." We can rewrite the family of filters presented in [2] in the form of a phase-compensated square-root filter, described in (16). In fact, Xia's Nyquist filters belong to the family of generalized raised-cosine filters in (32) with $\alpha \le 1/3$.

IV. Design Examples

In this section, we provide examples of Nyquist filter design using generalized raised-cosine filters. In practice, it is important that the transmitting and receiving filters be well approximated with short impulse responses. From this point of view, the standard raised-cosine filter is not necessarily the best choice for Nyquist filter design. We consider two design examples. First, a family of Nyquist pulses is designed such that these pulses have faster asymptotic decay than the raised-cosine filter impulse responses. In the second example, Nyquist filters are designed such that the intersymbol interference (ISI) caused by truncation of the transmitting and receiving filters is minimized.

A. Nyquist Filters with Smoother Spectra

It is a well-known result that if the amplitude response of a filter along with its first $(K-1)$ derivatives are all continuous but its Kth derivative is discontinuous, the filter impulse response asymptotically decays as $1/|t|^{K+1}$ [9]. Based on this result, the impulse response of a raised-cosine filter decays asymptotically as $1/|t|^3$. Using the generalized raised-cosine spectrum, we can design filters with higher rates of decay of their impulse responses. We use a family polynomials $P_n(x)$ to design the generalized raised-cosine spectra of (32) with higher degrees of continuity

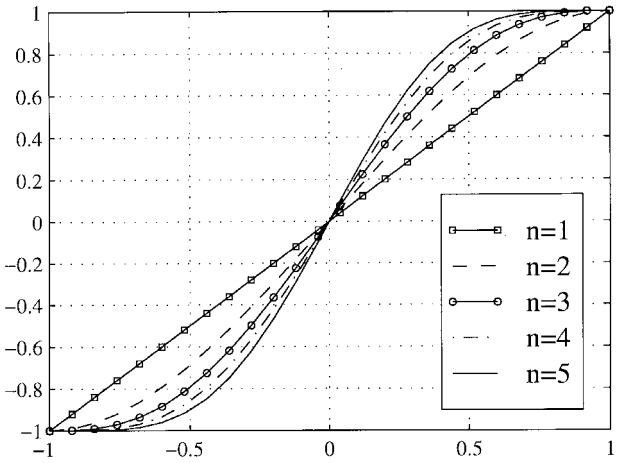

Fig. 6. Polynomials $P_n(x)$ to generate the generalized raised-cosine filter.

$$V(x) = \begin{cases} -1, & x < -1 \\ P_n(x), & -1 \le x \le 1 \\ 1, & x > 1 \end{cases} \quad (36)$$

where $V(x)$ specifies the phase compensator in (31). To satisfy condition (30), $P_n(x)$ should be an odd function of x

$$P_n(x) = \sum_{k=1}^{n} a_k \cdot x^{2k-1}$$

where a_k's are real-valued coefficients and a_n takes on a nonzero value. Furthermore, the coefficients a_k's are determined such that $V(x)$ and its first $(n-1)$ derivatives are continuous at $x = \pm 1$ which results in the following expression:

$$P_n(x) = \frac{\int_0^x (1-u^2)^{n-1}\,du}{\int_0^1 (1-u^2)^{n-1}\,du}, \qquad n = 1, 2, 3, \cdots. \quad (37)$$

The first derivative of $P_n(x)$ is a polynomial of degree $(2n-2)$ with $(n-1)$ repeated roots at $x = 1$ and by symmetry $(n-1)$ repeated roots at $x = -1$. Since the first derivative of $P_n(x)$ has no roots in $-1 < x < 1$ interval, $P_n(x)$ is monotonic in this interval. Fig. 6 illustrates the first five polynomials of this family.[1] The actual polynomials $P_n(x)$ are given in Table I. Note that $P_1(x)$ generates the standard raised-cosine filter. Using a Taylor series, we can show that the generalized raised-cosine spectrum corresponding to $P_n(x)$ has $(2n-1)$ continuous derivatives and its impulse response decays asymptotically as $1/|t|^{2n+1}$.

The rate of decay describes only the asymptotic behavior of the impulse response and does not characterize the impulse response for the first few lobes around the center. Fig. 7

[1] $P_1(x)$ and $P_3(x)$ correspond to examples presented by Xia [2].

TABLE I
COMPARISON OF SEVERAL GENERALIZED RAISED-COSINE FILTERS WITH $\alpha = 1$

n	$P_n(x)$	Decay	Eye-width
1	x	$\lvert t\rvert^{-3}$	1.000
2	$2^{-1}(-x^3+3x)$	$\lvert t\rvert^{-5}$	0.911
3	$2^{-3}(3x^5-10x^3+15x)$	$\lvert t\rvert^{-7}$	0.843
4	$2^{-4}(-5x^7+21x^5-35x^3+35x)$	$\lvert t\rvert^{-9}$	0.791
5	$2^{-7}(35x^9-180x^7+378x^5-420x^3+315x)$	$\lvert t\rvert^{-11}$	0.750

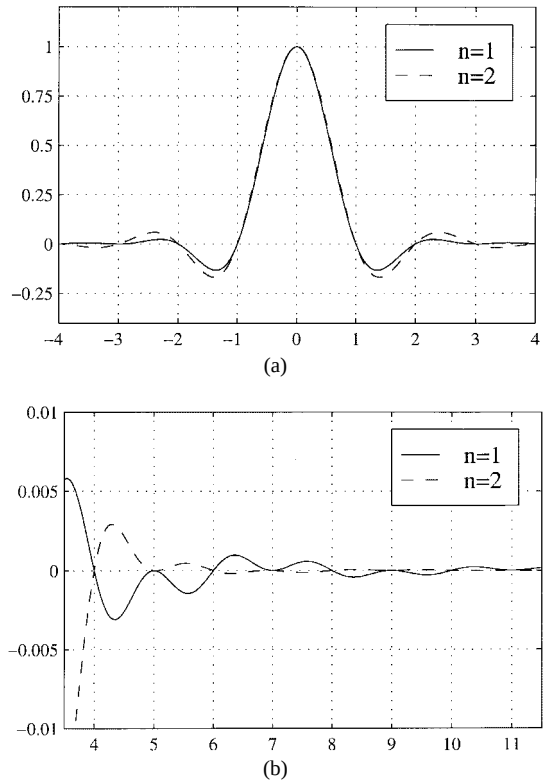

Fig. 7. Impulse responses of generalized raised-cosine filters generated by $P_1(x)$ and $P_3(x)$ are compared. (a) The main lobes of the impulse responses. (b) Extended scale view of the tails.

compares the impulse responses of two generalized raised-cosine filters generated from polynomials $P_1(x)$ and $P_2(x)$. The excess bandwidth in this case corresponds to $\alpha = 0.5$. Fig. 7(a) shows that for the first few lobes $|h_2(t)|$ is larger than $|h_1(t)|$. As shown in Fig. 7(b), only for the lobes farther away from the center is $h_2(t)$ smaller than $h_1(t)$.

Apart from the rate of decay of the filter-impulse response, there are other issues to be considered. Since timing recovery at the receiver is not always perfect, we encounter timing phase jitter. The eye-pattern diagram of a pulse shape can be used to assess the immunity of the pulse to timing phase jitter. Using polynomials given in Table I, we design five generalized raised-cosine filters with $\alpha = 1$ and normalized sampling period. Fig. 8 shows the inner boundaries of the binary eye diagrams associated with the impulse responses of these filters. As we increase the number of continuous derivatives of the spectrum, the width of the eye diagram decreases (see Table I).

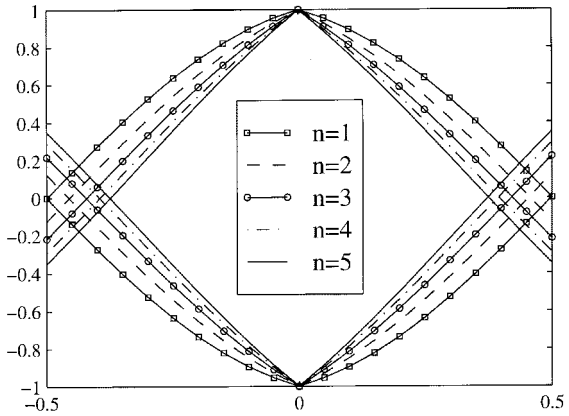

Fig. 8. Inner boundaries of the eye diagram for several generalized raised-cosine filters with $\alpha = 1$.

B. Nyquist Filters with Reduced ISI Due to Truncation

As shown in Section I, pulse shaping can be split between the transmitter and the receiver so that the overall response satisfies Nyquist's first criterion [see (5)]

$$g(t) = g_T(t) * g_R(t). \tag{38}$$

Truncating a Nyquist pulse does not affect its Nyquist zero-crossing property. However, the convolution of the truncated responses will in general no longer satisfy Nyquist's first criterion.

Here we use generalized raised-cosine filters to design Nyquist filters with minimized ISI due to impulse-response truncation. To study the effect of truncating the impulse response of the square-root filter, we consider the following conditions.

- We assume that the compensated square-root generalized raised-cosine filters are used at the transmitter and the receiver. In this example we assume the channel is ideal with additive noise.
- To specify the generalized raised-cosine filter of (32), we define $V(x)$ as follows:

$$V(x) = \begin{cases} -1, & x < -1 \\ P(x), & -1 \le x \le 1 \\ 1, & x > 1 \end{cases} \tag{39}$$

where $P(x)$ is a polynomial defined as

$$P(x) = \frac{\displaystyle\int_0^x (1+p_1u^2)(1+p_2u^2)\,du}{\displaystyle\int_0^1 (1+p_1u^2)(1+p_2u^2)\,du}. \tag{40}$$

To obtain a monotonic function $V(x)$, both p_1 and p_2 should be greater than or equal to -1. Note that for $p_1 = p_2 = 0$, $P(x) = x$, which generates the phase compensated standard raised-cosine filter. For $p_1 = p_2 = -1$, $P(x) = P_3(x)$ as defined in (37).

- To calculate samples of the impulse response of the transmitting and receiving filters, we evaluate (34) numerically. Each impulse response is calculated for $N \cdot M$

TABLE II
NYQUIST FILTER DESIGN TO REDUCE ISI DUE TO TRUNCATION

α	$P(x)$	N	Truncation effects: Minimized D_{peak}	Truncation effects: Standard D_{peak}
0.10	$0.4799x^5 + 0.3827x^3 + 0.1373x$	14	0.125	0.216
0.15	$0.3147x^5 + 0.4259x^3 + 0.2594x$	10	0.104	0.192
0.25	$0.2951x^5 + 0.4269x^3 + 0.2780x$	6	0.089	0.194
0.50	$-0.0105x^5 - 0.1775x^3 + 1.1879x$	6	0.015	0.046
0.75	$-0.0145x^5 - 0.2122x^3 + 1.2267x$	4	0.011	0.052
1.00	$0.0192x^5 + 0.1844x^3 + 0.7964x$	4	0.004	0.010

points where M is the up-sampling ratio and N is the number of lobes in each truncated impulse response. Numerical results are presented for $M = 20$.

- The overall impulse response is determined by convolving the impulse responses of the truncated transmitting and receiving filters.
- To measure the ISI caused by truncation, we use the peak distortion criterion [10]

$$D_{\text{peak}} = \frac{1}{h(0)} \sum_{\substack{n=-N \\ n\neq 0}}^{N} |h(nT_s)| \tag{41}$$

where $h(t)$ is the overall impulse response.

Table II shows the results for several values of normalized excess bandwidth α. In each case, the parameters $p1$ and $p2$ are found using an optimization procedure to minimize D_{peak}. The corresponding polynomial $P(x)$ is given in the second column of the table. For each α, two values of D_{peak} are presented. The "minimized D_{peak}" value corresponds to the filter generated by $P(x)$ and the "standard D_{peak}" value corresponds to the filter generated by $P(x) = x$, which is a phase compensated square-root of the standard raised-cosine filter. In all cases the optimized filters produce less ISI due to truncation of the impulse responses.

To calculate probabilities of error, we assume a white Gaussian additive noise corrupts the transmitted signal. An upper bound for probability of error for binary data can be found in terms of D_{peak} [10]

$$\hat{P}_e = Q\left(\frac{1 - D_{\text{peak}}}{\sigma}\right) \tag{42}$$

where σ is the standard deviation of the noise and $Q(x) = (1/\sqrt{2\pi}) \int_x^\infty e^{-t^2/2}\, dt$. For example, consider the second row of Table II. If the probability of error with zero ISI ($D_{\text{peak}} = 0$ for $N = \infty$) is 10^{-6}, then with $D_{\text{peak}} = 0.104$, the worst case bound for the probability of error is $\hat{P}_e = 1.02 \times 10^{-5}$. For $D_{\text{peak}} = 0.192$, we obtain $\hat{P}_e = 6.13 \times 10^{-5}$.

Table II also shows that for smaller values of α, truncating the filter-impulse response causes a larger distortion. Comparing different rows of the table, we notice that filters with smaller excess bandwidth have larger ISI due to truncation even though they have larger truncation lengths.

V. CONCLUDING REMARKS

We have shown that any zero-phase bandlimited Nyquist filter with normalized excess bandwidth can be split into two cascaded Nyquist-matched filters. Each filter consists of the square-root of the overall response along with a phase compensator. We have expressed the phase compensator in terms of the square-root magnitude response of the overall filter.

The phase compensation can be applied to the square-root of a standard raised-cosine spectrum. The required phase response in this case is a simple piecewise linear function. For standard raised-cosine filter with $\alpha = 1$, the square-root filter satisfies Nyquist's first criterion, provided an appropriate time delay is added to the impulse response.

Using the phase-compensation technique, we have extended the family of raised-cosine filters to a more general family of Nyquist filters. Compared to the standard raised-cosine spectrum, the family of generalized raised-cosine filters provides more flexibility for designing Nyquist filters. As an example, we designed a family of Nyquist filters with smoother spectra. The impulse responses of these filters have higher asymptotic rates of decay. We also designed transmitting and receiving filters such that when we truncate the impulse responses of these filters, the overall impulse response has a reduced ISI.

APPENDIX A
INNER BOUNDARIES OF THE EYE PATTERN FOR THE SQUARE-ROOT FILTER

To find the lower boundaries of the eye pattern diagram of the square-root full raised-cosine filter, we first determine the maximum ISI for a PAM signal. From (1) we obtain

$$x(\tau) = a_0 g(\tau) + \sum_{\substack{n=-\infty \\ n\neq 0}}^{\infty} a_k g(\tau - n) \tag{43}$$

where τ is the time offset relative to the sampling instances nT_s. The second term in this equation is due to ISI. In the case of binary PAM signal with $a_k = \pm 1$, the maximum ISI for a Nyquist pulse is calculated as

$$D(\tau) = \sum_{\substack{n=-\infty \\ n\neq 0}}^{\infty} |g(\tau - n)|. \tag{44}$$

Therefore, the eye-pattern boundaries are

$$\begin{aligned} &\text{lower boundaries: } = \pm(g(\tau) - D(\tau)) \\ &\text{upper boundaries: } = \pm(g(\tau) \pm D(\tau)). \end{aligned} \tag{45}$$

Substituting (22) into (44), we obtain

$$g(\tau) - D(\tau) = \frac{-\cos(2\pi\tau)}{4\pi(\tau + 1/4)(\tau - 1/4)} - \frac{\cos(2\pi\tau)}{4\pi} \cdot \sum_{\substack{n=-\infty \\ n\neq 0}}^{\infty} \left| \frac{1}{(\tau + n + 1/4)(1/4 - \tau - n)} \right|. \tag{46}$$

For $|\tau| \le 1/4$, the above expression simplifies to

$$g(\tau) - D(\tau) = -\frac{\cos(2\pi\tau)}{4\pi} \sum_{n=-\infty}^{\infty} \frac{1}{(\tau+n+1/4)(\tau+n-1/4)}, \quad \text{for } |\tau| \le \tfrac{1}{4}. \tag{47}$$

Consider the following identity:

$$\sum_{k=-\infty}^{\infty} \frac{1}{(x+k+1/4)(x+k-1/4)} = \frac{-4\pi}{\cos(2\pi x)}. \tag{48}$$

Therefore, the lower boundaries of the eye pattern are

$$\pm(g(\tau) - D(\tau)) = \pm 1, \qquad \text{for } |\tau| \le \tfrac{1}{4}. \tag{49}$$

APPENDIX B
THE IMPULSE RESPONSE OF $H_{\text{sqrt}}(f)$

To obtain the impulse response given in (34), we note that $H_{\text{sqrt}}(f)$, as defined in (32), has Hermitian symmetry. The inverse Fourier transform of $\sqrt{T_s}H_{\text{sqrt}}(f)$ can be written as

$$\begin{aligned}
&\mathcal{F}^{-1}\left\{\sqrt{T_s}H_{\text{sqrt}}(f)\right\} \\
&\quad = 2T_s \int_0^{(1-\alpha)/2T_s} \cos(2\pi f t)\, df \\
&\qquad + 2T_s \int_{(1-\alpha)/2T_s}^{(1+\alpha)/2T_s} \cos(\phi(f)) \cdot \cos(\phi(f) + 2\pi f t)\, df \\
&\quad = 2T_s \int_0^{(1-\alpha)/2T_s} \cos(2\pi f t)\, df \\
&\qquad + T_s \int_{(1-\alpha)/2T_s}^{(1+\alpha)/2T_s} \cos(2\pi f t)\, df \\
&\qquad + T_s \int_{(1-\alpha)/2T_s}^{(1+\alpha)/2T_s} \cos(2\phi(f) + 2\pi f t)\, df
\end{aligned} \tag{50}$$

where $\phi(f)$ is defined in (31). The first two terms of (50) can be combined as follows:

$$\begin{aligned}
&2T_s \int_0^{(1-\alpha)/2T_s} \cos(2\pi f t)\, df + T_s \int_{(1-\alpha)/2T_s}^{(1+\alpha)/2T_s} \cos(2\pi f t)\, df \\
&\quad = \operatorname{sinc}\left(\frac{t}{T_s}\right) \cdot \cos\left(\frac{\pi t \alpha}{T_s}\right).
\end{aligned} \tag{51}$$

By introducing a new variable $x = (2T_s/\alpha)(f - (1/2T_s))$, we simplify the third integral in (50) to

$$\begin{aligned}
&T_s \int_{(1-\alpha)/2T_s}^{(1+\alpha)/2T_s} \cos(2\phi(f) + 2\pi f t)\, df \\
&\quad = \frac{\alpha}{2} \int_{-1}^{1} \sin\left(\frac{\pi}{2} V(x) - \frac{\pi t \alpha}{T_s} x + \frac{\pi t}{T_s}\right) dx \\
&\quad = \alpha \sin\left(\frac{\pi t}{T_s}\right) \int_0^1 \cos\left(\frac{\pi}{2} V(x) - \frac{\pi t \alpha}{T_s} x\right) dx.
\end{aligned} \tag{52}$$

Combining (51) and (52), we obtain the result as given in (34).

REFERENCES

[1] J. G. Proakis, *Digital Communications*, 3rd ed. New York: McGraw-Hill, 1995.

[2] X.-G. Xia, "A family of pulse-shaping filters with ISI-free matched and unmatched filter properties," *IEEE Trans. Commun.*, vol. 45, pp. 1157–1158, Oct. 1997.

[3] E. Ayanoglu, N. R. Dagdeviren, G. D. Golden, and J. E. Mazo, "An equalizer design technique for the PCM modem: A new modem for the digital public switched network," *IEEE Trans. Commun.*, vol. 46, pp. 763–774, June 1998.

[4] P. A. Humblet and M. G. Troulis, "The information driveway," *IEEE Commun. Mag.*, vol. 34, pp. 64–68, Dec. 1996.

[5] N. Sheikholeslami and P. Kabal, "Linear time varying precoder applied to ISI channel," in *IEEE Pacific Rim Conf. Communications, Computers and Signal Processing*, 1997, pp. 36–39.

[6] R. A. Gibby and J. W. Smith, "Some extensions of Nyquist's telegraph transmission theory," *Bell Syst. Tech. J.*, vol. 44, pp. 1487–1510, Sept. 1965.

[7] J. A. C. Bingham, *The Theory and Practice of MODEM Design.* New York: Wiley, 1988.

[8] E. A. Lee and D. G. Messerschmitt, *Digital Communication.* Boston, MA: Kluwer Academic, 1994.

[9] P. Kabal and S. Pasupathy, "Partial response signaling," *IEEE Trans. Commun.*, vol. 23, pp. 921–934, Sept. 1975.

[10] R. D. Gitlin, J. F. Hayes, and S. B. Weinstein, *Data Communications Principles.* New York: Plenum, 1992.

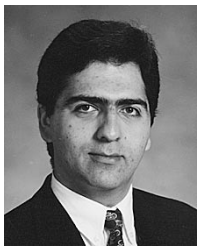

Nader Sheikholeslami Alagha received the B.Sc. degree in electrical engineering from Tehran University, Tehran, Iran, in 1990 and the M.A.Sc. degree from the University of Waterloo, ON, Canada, in 1994. He is currently completing the requirements for the Ph.D. degree in electrical and computer engineering at McGill University, Montreal, PQ, Canada.

He has been a part-time faculty Lecturer at the Department of Electrical and Computer Engineering, McGill University, since 1996. His research interests are in the field of digital signal processing applied to data transmission.

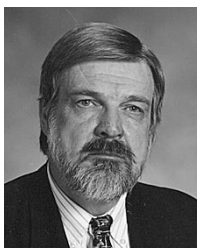

Peter Kabal (S'70–M'75) received the B.A.Sc., M.A.Sc., and Ph.D. degrees in electrical engineering from the University of Toronto, Toronto, ON, Canada. He is currently a Professor in the Department of Electrical Engineering, McGill University, Montreal, PQ, and a Visiting Professor at INRS-Telecommunications (a research institute affiliated with the Université du Québec), Verdun, PQ. His current research interests focus on digital signal processing as applied to speech coding, adaptive filtering, and data transmission.